iScience, Volume *24*

Supplemental information

Analysis of biological noise in the flagellar length control system

David Bauer, Hiroaki Ishikawa, Kimberly A. Wemmer, Nathan L. Hendel, Jane Kondev, and Wallace F. Marshall

Supplemental Information

Transparent Methods

Strains, media, and imaging

All strains were obtained from the Chlamydomonas Resource Center (University of Minnesota, St. Paul, MN), with the exception of *lf4* mutant strain V13 which was provided by Gregory Pazour, UMASS Medical Center. The *lf4* mutation was confirmed in this strain by PCR (data not shown). For asynchronous culture, cells were grown in 2mL cultures in TAP media (Harris, 1989) under continuous illumination. Cultures arrested in G1 were obtained by growing cells in M1 media for 2 days in continuous illumination and then switching them to continuous darkness for 24 hours. Gametes were grown overnight in M-N media.

To measure flagellar length in fixed cells, cells were fixed in 1% glutaraldehyde, and imaged using DIC optics with an Olympus 60x air lens and an air condenser on a DeltaVision 3D microscopy system. Three dimensional data was collected using a 0.2 μm step in the Z-axis. Lengths were then measured by tracing the flagella in three dimensions using the DeltaVision distance measuring function with the multi-segment length calculation method.

To measure flagellar length fluctuations in live cells, cultures were grown in TAP media at 21ºC in constant light on a roller drum. For embedding live cells, 1% w/v agarose was melted in TAP media and cooled to 41ºC. A square of Vaseline was made on a glass slide, then 5μL of culture was mixed with 20μL agarose in TAP within the square. The slide was then inverted over a coverslip, compressing the agarose in TAP into a flat, square pad. The cells were allowed to recover at room temperature in light for 2 hours to overnight, then imaged. The slide was

imaged using DIC microscopy on a Deltavision microscopy system, at room temperature in ambient light. Embedded cells were imaged using a 100x oil immersion lens (NA 1.40 PlanApo) with a z step size of 0.2 microns. One z stack was taken through the entire cell every 10 minutes for 2 hours. The time interval for data acquisition was chosen based on the fact that flagellar length changes during flagellar regeneration take place on the times scale of tens of minutes. The length of the flagella was measured using the length measurement function in the Deltavision microscope software, which allows the user to step up and down through the Z-stack, clicking on a series of points. The software then adds up the length of line segments joining successive points, taking into account the voxel size in X, Y, and Z.

Measuring flagellar length in live cells before and after pH shock

Two different apparatus were used separately to image flagella of individual *Chlamydomonas* cells during and after pH shock. In the first approach (**Figure 3A, S1A,B**), we used the CellASIC ONIX Microfluidic System (EMD Millipore, Hayward, CA). Cultured cells were loaded into the Microfluidic Chlamydomonas Trap Plate (C04A-01, EMD Millipore) and imaged on an inverted microscope (Ti-E Microscope, Nikon, Tokyo, Japan) with a 40× objective (Plan Fluor, 0.75 NA, Nikon) and an sCMOS camera (ORCA-Flash4.0, Hamamatsu Photonics, Hamamatsu, Japan) at 25ºC. Cells were held in the microfluidic chamber in the plate by perfusing with TAP media at 5 psi and imaged by differential interference contrast (DIC) with 5 z-stacks at 0.9 µm intervals. To remove flagella from cells, we performed the pH shock method in the microfluidic chamber. Cells in the microfluidic chamber were deflagellated by perfusing with TAP media (pH 4.5, adjusted with acetic acid) for 1 minute, then neutralized by perfusing

with TAP media (pH 9.0, adjusted with potassium hydroxide) for 30 seconds. After neutralization, the chamber was perfused with normal TAP media (pH 7.0) during the imaging. Cells were imaged every 10 minutes for 2 hours after pH shock deflagellation. Flagella were measured by hand-tracing in ImageJ (NIH, Bethesda, MA).

The long length of tubing in the CellASIC system raised concerns about the speed of solution exchange. We therefore implemented a second approach, by designing and fabricating a microfluidic device based on a serpentine channel (**Supplementary Figure S1C**) designed to allow rapid solution exchange while trapping cells. A single device is capable of immobilizing approximately 100 cells to a narrow z-plane (15 μm). The trapped cells are stable for many hours (>24), undergo cell division, and regenerate flagella. Unlike the CellASIC device, the serpentine channels are not suitable for imaging by DIC because flagella often lie near the channel wall and are thus difficult to image. We therefore used fluorescent imaging of cells expressing a flagellar marker. FAP20GFP (Yanagisawa et al,. 2014) cells were synchronized via a 14/10 light/dark cycle and hand injected using a syringe and a tube into the device until all traps were

occupied. Constant flow was then established by attaching a syringe pump with normal and low-pH M1 media to the loaded device. A valve (Chrom Tech V-100D) was used to switch from normal to low-pH media with minimal lag time (**Supplemental Figure S1D**). The loaded device was mounted on a custom built OMX microscope (Dobbie et al,. 2011) with a 100X objective lens. An initial 3D-measurement (16 μm z-stack, axial spacing of 0.2 μm) was taken of flagellar length in the GFP channel (65μW @ 455nm at the sample). Cells were then pH shocked via switching to low-pH media for 60 seconds and returning to normal-pH media (**Supplementary**

Figure S1D). Two hours after pH shock, cells were imaged again in the GFP channel for a final 3D length measurement. Length measurements were made by hand in ImageJ. XY and Z measurements were combined to compute overall length (**Supplementary Figure S1E,F**).

Estimation of measurement noise

We used time-lapse imaging to obtain two separate estimates for measurement error. First, as plotted by the black data-points in **Figure 1C**, we imaged cells fixed in glutaraldehyde at multiple sequential time points and then calculated the mean squared difference in length. As expected for measurement errors that are uncorrelated with each other, the slope of the best fit line to this data was less than $5x10^{-5}$, showing that the difference in measured length was independent of time lag. The average value of the mean squared difference in length was 0.0438 square microns, corresponding to an average measurement error of 0.2 microns.

As an alternative measure, we analyzed the fluctuations in live cells and calculated the mean squared change in difference between L_1 and L_2, and plotted this versus time. This plot gave a roughly linear behavior for the first several time points. The mean squared change in length is the sum of two contributions – length fluctuations, which for a random-walk type of motion would be proportional to the time lag, and measurement error, which is a constant at each time point and thus independent of time lag. For a one-dimensional random walk (such as that executed by the difference in length between the two flagella), the Y intercept of this plot should correspond to 4 times the mean squared measurement error in each measurement. We therefore fitted a straight line to the first ten time points and obtained a Y intercept of 0.597 microns squared. We thereby obtain an estimated measurement error of 0.39 microns.

We thus obtain two independent estimates of measurement error, both of which are on the same order of magnitude as the XYZ voxel edge length, much smaller than the observed variations in length between flagella. The second estimate is larger than the first, possibly because in living cells embedded in agarose, small motions of the flagella may contribute to measurement error.

Modeling flagellar length noise using the balance-point length control model

We have previously described a simple model for length control of cilia and flagella that has been termed the balance-point model. This model is based on observations that the axonemal microtubules undergo continuous turnover at their plus-ends, with disassembly taking place at a constant rate regardless of length, and assembly taking place at a rate limited by IFT (Marshall and Rosenbaum, 2001). A key component of the model is the hypothesis that intraflagellar transport is length-dependent. This dependency arises because the rate at which IFT particles enter the flagellum is proportional to 1/L (Marshall and Rosenbaum, 2001; Marshall et al., 2005; Engel 2009; Ludington 2013). The mechanistic reason for the 1/L dependence of IFT entry on length is not currently understood, although several models have been proposed (Ludington 2015; Ishikawa 2017b; Hendel 2018). Under the assumption that assembly is rate-limited by transport, it follows that the assembly rate is proportional to 1/L while measurements show that the disassembly rate is independent of length (Marshall and Rosenbaum 2001). Therefore, the assembly rate versus length curve will intersect the disassembly versus length curve at a unique value of the length, which reflects the steady state length of the flagella. The model presented here ignored a number of potential complications

including the possibility that tubulin loading onto IFT particles may be regulated as a function of length (Craft 2015) and the fact that precursor production inside the cell body is actively regulated as a function of flagellar dynamics.

Following our previous formulation of the balance-point length control model, we define three parameters, A, P, and D. Parameter A describes the efficacy of intraflagellar transport and encapsulates the speed of the IFT particles, the number of IFT particles in a flagellum (a quantity known to be independent of length), and the cargo carrying-capacity of the particles. The parameter P describes the total pool of flagellar protein in a cell, including protein incorporated into the two flagella as well as unincorporated precursor stored in the cytoplasm (Rosenbaum et al., 1969). Parameter D describes the rate of flagellar disassembly. We have previously estimated values for these parameters in wild-type cells: D ~ 0.011 μm/min (measured from the rate of shortening in *fla10* mutant cells), A ~ 0.0055 μm/min, and P ~ 40 μm (measured from the ratio of flagellar lengths before and after regeneration in the presence of cycloheximide (Marshall and Rosenbaum, 2001)). Note that the pool size is expressed in units of length, the conversion factor being the quantity of protein required to assemble a 1 μm segment of the axoneme.

The balance-point model can be encapsulated by a pair of coupled differential equations, one for each of the two flagellar lengths L_1 and L_2:

$$\dot{L}_1 = f(L_1, L_2) = A\frac{(P - L_1 - L_2)}{L_1} - D$$

$$\dot{L}_2 = g(L_1, L_2) = A\frac{(P - L_1 - L_2)}{L_2} - D$$

for which the steady state solution is:

$$L_1 = L_2 = L_{ss} = \frac{P}{2 + \frac{D}{A}}$$

With the estimated parameter values given above, this predicts a steady state length of 10 μm.

In order to ask whether parameter changes that increase the steady-state length would be predicted to increase noise, we performed stochastic simulations of the above system of two equations, modified such that either one of the three parameters A, D, or P, was changed at regular intervals by sampling from a Gaussian distribution centered at the specified average value of the parameter in question. The simulation was initiated at the steady-state length given by our analytical solution above, and then run for 10,000,000 iterations using the Euler method with a time step corresponding to 0.01 minutes. New values of the fluctuating parameter were chosen every 1000 iterations (corresponding to 10 minutes to roughly reflect the order of magnitude time scale of observed fluctuations). Flagellar lengths were constrained to be non-negative in the simulation. Uncorrelated variation was computed based on the simulated length time course of the two flagella. The variance of the Gaussian used for representing parameter fluctuation was adjusted so that the simulated uncorrelated variation approximately matched the measurements from wild-type cells. For each case of fluctuations applied to D or to A, we varied all three parameters independently so as to increase length from 10 to 20 microns, and plotted the uncorrelated variation normalized by the uncorrelated

variation calculated in simulations using wild-type parameter values. These results are plotted in **Figure 5D-E**.

In addition to simulating the effect of parameter fluctuations, we also simulated the effect of adding a fluctuation term to the net growth rate of each flagellum. To do this, during the simulations as described above, each flagellum was assigned a growth rate perturbation whose value was chosen from a Gaussian distribution of zero mean, with new values chosen every 1000 iterations. Again, the three parameter values A, D, and P were systematically varied to produce longer steady state lengths, and in each case the uncorrelated variation was computed over the course of the simulation. These results were plotted in **Figure 5F**.

In order to obtain an analytical model that accounts for the increased uncorrelated variation seen when the decay parameter D is reduced in the above growth-rate fluctuation model, we employ a linear noise analysis to model how the system restores itself back to the steady-state length following small deviations, and then consider the effect of this restoration on a system in which the growth rate is randomly perturbed.

We begin our small-signal noise analysis by introducing two variables:

$$x = L_1 - L_2$$
$$y = L_1 + L_2 - 2L_{ss}$$

The new variables x and y correspond to the differences in flagellar length within one cell and the cell-to-cell variation in average length, respectively, that will result from a noise source applied to one of the two flagella, i.e., the response to an intrinsic noise source in one flagellum. We next consider the rate at which a deviation in L_1 at time t=0 will gradually be eliminated to bring the system back to the steady state solution. Initially this deviation would

alter both x and y, but then over time the system will restore the flagellar lengths to their steady-state values. To determine how fast this restoration will occur, we linearize the system, as follows. First, we note that x and y can be expressed in terms of the deviations from the steady state in L_1 and L_2 as follows:

$$u = L_1 - L_{ss}$$
$$v = L_2 - L_{ss}$$
$$x = u - v$$
$$y = u + v$$

Assuming the perturbations are small, u and v will be close to zero. The rate of change of the deviations u and v is approximated by the Jacobian:

$$\begin{pmatrix} \dot{u} \\ \dot{v} \end{pmatrix} = \begin{pmatrix} \left.\frac{\partial f}{\partial L_1}\right|_{L_1=L_2=L_{ss}} & \left.\frac{\partial f}{\partial L_2}\right|_{L_1=L_2=L_{ss}} \\ \left.\frac{\partial g}{\partial L_1}\right|_{L_1=L_2=L_{ss}} & \left.\frac{\partial g}{\partial L_2}\right|_{L_1=L_2=L_{ss}} \end{pmatrix} \begin{pmatrix} u \\ v \end{pmatrix}$$

Evaluating the partial derivatives around the steady-state value $L_1=L_2=L_{ss}$ we obtain the linearized system:

$$\begin{pmatrix} \dot{u} \\ \dot{v} \end{pmatrix} = A \begin{pmatrix} \frac{(L_{ss}-P)}{L_{ss}^2} & -\frac{1}{L_{ss}} \\ -\frac{1}{L_{ss}} & \frac{(L_{ss}-P)}{L_{ss}^2} \end{pmatrix} \begin{pmatrix} u \\ v \end{pmatrix}$$

We then express the behavior of x and y in the linear approximation according to

$$\dot{x} = \dot{u} - \dot{v}$$
$$\dot{y} = \dot{u} + \dot{v}$$

This substitution yields, finally, a pair of uncoupled differential equations for x and y:

$$\dot{x} = u\left(\left.\frac{\partial f}{\partial L_1}\right|_{L_1=L_2=L_{ss}} - \left.\frac{\partial g}{\partial L_1}\right|_{L_1=L_2=L_{ss}}\right) + v\left(\left.\frac{\partial f}{\partial L_2}\right|_{L_1=L_2=L_{ss}} - \left.\frac{\partial g}{\partial L_2}\right|_{L_1=L_2=L_{ss}}\right)$$
$$= (u-v)\left\{A\frac{(L_{ss}-P)}{L_{ss}^2} + \frac{A}{L_{ss}}\right\}$$
$$= \left\{A\frac{(L_{ss}-P)}{L_{ss}^2} + \frac{A}{L_{ss}}\right\}x$$

and

$$\dot{y} = u\left(\left.\frac{\partial f}{\partial L_1}\right|_{L_1=L_2=L_{ss}} + \left.\frac{\partial g}{\partial L_1}\right|_{L_1=L_2=L_{ss}}\right) + v\left(\left.\frac{\partial f}{\partial L_2}\right|_{L_1=L_2=L_{ss}} + \left.\frac{\partial g}{\partial L_2}\right|_{L_1=L_2=L_{ss}}\right)$$
$$= \left\{A\frac{(L_{ss}-P)}{L_{ss}^2} - \frac{A}{L_{ss}}\right\}y$$

we define constants:

$$\alpha = A\frac{(L_{ss}-P)}{L_{ss}^2} + \frac{A}{L_{ss}}$$
$$\beta = A\frac{(L_{ss}-P)}{L_{ss}^2} - \frac{A}{L_{ss}}$$

hence:

$$\dot{x} = \alpha x$$
$$\dot{y} = \beta y$$

which, by inspection, have exponential functions as their solutions:

$$x(t) = x(0)e^{\alpha t}$$
$$y(t) = y(0)e^{\beta t}$$

We now consider what happens if we add random fluctuations to the system. We model intrinsic fluctuations by adding a noise term to the equation governing the rate of change of x, thus:

$$\dot{x} = \alpha x + \sigma\eta$$

where σ denotes the magnitude of the fluctuations (in microns) and η denotes Gaussian white noise with zero mean and variance 1. By adding the white noise term to the rate of change of x, we represent fluctuations in the assembly and disassembly processes taking place at the flagellar tip, for example due to stochastic variation in microtubule polymerization and depolymerization. The stationary solution to this equation (Honerkamp, 1994; Van Kampen, 1992) has a mean of 0 and a mean squared value of:

$$\left\langle x^2 \right\rangle = \frac{\sigma^2}{2\alpha}$$

We assume that σ is the same for wild type and mutant cells. Hence the mean squared difference in length between the two flagella should be proportional to $1/\alpha$. Substituting the value of α derived above and then using the value of L_{ss} in terms of the three parameters A, D, and P, we obtain

$$\left\langle \left(L_1 - L_2\right)^2 \right\rangle \sim \frac{1}{\left\{ A\frac{L_{ss} - P}{L_{ss}^2} + \frac{A}{L_{ss}} \right\}} = \frac{P}{D\left(2 + {}^{D}\!/_{A}\right)}$$

Using this expression to calculate the uncorrelated variation, we obtain

$$\eta_{int}^2 = \frac{\langle (L_1 - L_2)^2 \rangle}{2\langle L_{ss} \rangle^2} = \frac{P}{D\left(2 + {}^{D}\!/_{A}\right)} \frac{\left(2 + {}^{D}\!/_{A}\right)^2}{2P^2} = \frac{2 + {}^{D}\!/_{A}}{2DP} = \frac{1}{DP} + \frac{1}{2AP}$$

Which is given as Equation (5) in the Results section.

Measurement of swimming speed versus flagellar length by high-speed video

To obtain simultaneous measurements of swimming speed and flagellar lengths for **Figure 6A** we mounted cells between a slide and coverslip supported by a 1 mm thick Vaseline ring, and imaged the cells on a Zeiss Axiovert 200M microscope with a 40X air objective lens using DIC optics and an infrared-blocking filter, collecting data with a Phantom MiroEx4-1024MM video camera at a frame rate of 1000 fps, exposure time 998 μSec. Cells were imaged at a dilution that ensured at most one or two cells per field of view. Following collection of each dataset, individual cells were manually tracked for 10 cycles of flagellar beating, marking the position of the cell at the beginning and end of this period. The difference in position divided by the elapsed time was taken as the average swimming speed. Since our data collection was only two-dimensional, many cells swam out of focus during the imaging and those images were discarded. Only cells for which the flagella remained in focus through the entire 10 beat cycles were used for distance measurements. In order to cover a wider range of lengths, we measured both wild-type cells and *lf1* mutant cells, which frequently have unequal lengths and which span a range of short and long lengths. Swimming speed for *lf1* mutants whose flagella are in the wild-type range are not statistically different from speeds of wild-type cells. Distance measurements of swimming and length measurement of flagella were performed using the Phantom Miro software. Contour plots of swimming speed were generated by calculating average swimming speeds among data points within a moving square window of side length 2 microns. The length range (0-16 microns) was divided into 50 intervals, and the window scanned across all combinations of intervals for L1 and L2. The range of 0-16 microns was chosen because among the cells randomly sampled for image analysis, most fell within this range, and there were not enough datapoints outside that range to obtain good estimates for

the contour plot. For windows in which no data points were available, the closest data point (in terms of the Euclidean distance with L1 and L2 as coordinates) was taken as the value for the center of the window. The data was then smoothed with a 4x4 moving average filter to produce the final plot. 15 equally spaced contour levels were used between the maximum and minimum speeds.

Measurement of gliding versus flagellar length

Cells were grown in TAP media and loaded onto a coverslip within a 2 mm thick Vaseline ring and inverted over a slide. As with swimming speed, measurements were performed using both wild-type and lf1 mutant cells, in order to obtain a wider range of flagellar lengths. Cells were imaged using a 20x objective with DIC optics. 25 images were collected at a rate of 1 image every 10 seconds. The total distance travelled by a cell was then calculated as the distance between the start and end point of the time series and the velocity calculated by dividing this distance by the total data collection time. The number of directional reversals for each cell during the entire time-course was determined by visual inspection. Plots of gliding velocity were generated using the same procedure as for swimming speed, except that the final smoothing used a 10x10 moving average filter.

Supplemental References

Dobbie IM, King E, Parton RM, Carlton PM, Sedat JW, Swedlow JR, Davis I. 2011. OMX: a new platform for multimodal, multichannel wide-field imaging. *Cold Spring Harbor Protoc.* **2011**, 899-909.

Harris EH. 1989. *The Chlamydomonas sourcebook*. Academic Press, San Diego, CA 780 pp.

Honerkamp J. *Stochastic dynamical systems*. 1994. Wiley-VCH, New York, NY. 535 pp.

Van Kampen NG. 1992. *Stochastic processes in physics and chemistry*. North Holland Press, Amsterdam.

Yanagisawa HA, Mathis G, Oda T, Hirono M, Richey EA, Ishikawa H, Marshall WF, Kikkawa M, Qin H. 2014. FAP20 is an inner junction protein of doublet microtubules essential for both the planar asymmetrical waveform and stability of flagella in Chlamydomonas. *Mol. Biol. Cell* **25**, 1472-83.

Supplemental Figure Legends

Supplemental Figure S1 related to Figure 3. Additional data for Figure 3 about testing the cell body contribution to length variation. (**A**) Cells growing in commercial CellASIC chamber, based on a previously published design (Ludington 2012). (**B**) Length measurements before and after regeneration in *ptx1* mutant cells in CellASIC chamber (r=0.41; p=0.016; n=34). For

this measurement, an outlier cell whose starting flagellar length was less than 7 microns was removed. (**C**) Design of alternative microfluidic trap for Chlamydomonas based on a serpentine channel. Lower image shows cells trapped by flow through holes in the serpentine channel. (**D**) pH change profile measured in serpentine microfluidic device. (**E**) Length measurements before and after regeneration in wild-type cells in serpentine fluidic device. To avoid potential confusion between the two flagella, both flagella lengths from one cell were averaged to compute correlation coefficients (r= 0.41; p=0.013; n=36). (**F**) As an additional test for cell-cell length variation, lengths before and after regeneration were compared between the same cell (blue) and randomly chosen cells (orange), and the mean squared difference in length recorded. The plot shows the histograms that result, indicating that comparison of flagellar lengths before vs. after regeneration in unrelated cells shows a greater difference than comparisons taken from the same cell.

Supplemental Figure S2 related to Figure 6. Additional data for Figure 6 regarding effects of flagellar length on motility. **(A)** Swimming speed versus flagellar length, with lengths of gametes superimposed as white boxes. Swimming speed data is the same as Figure 6A, but the gamete data-points illustrate that the length distribution of gamete flagella is better matched to the regime of optimal swimming. (**B**) Reversal frequency during gliding plotted versus flagellar lengths. White corresponds to maximum frequency of reversal, black minimum. The most reversals occur for cells with flagella of equal lengths, while increased length disparity correlates with decreased reversals.

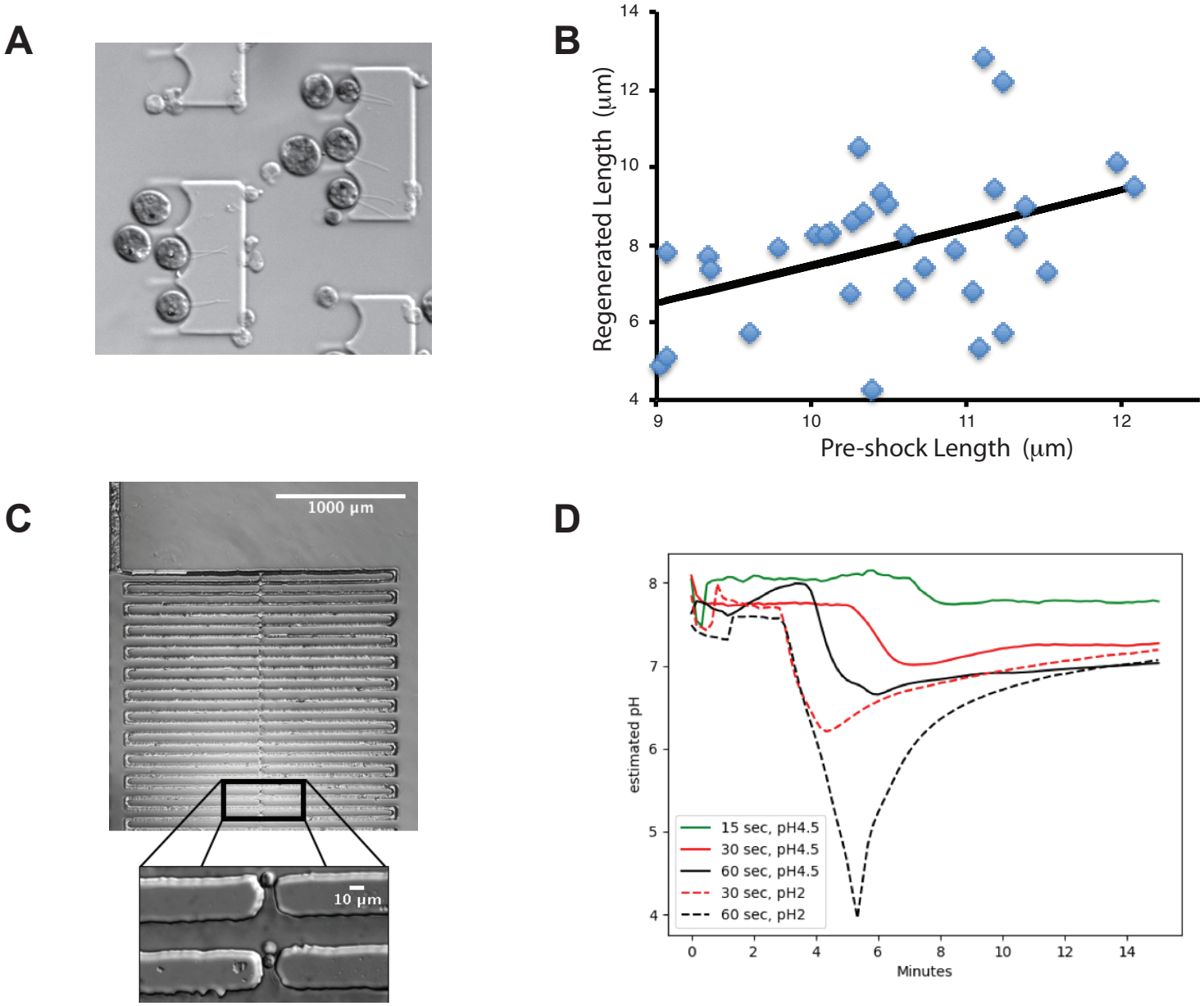
A
B
Regenerated Length (µm)
Pre-shock Length (µm)
C
1000 µm
10 µm
D
estimated pH
Minutes
15 sec, pH4.5
30 sec, pH4.5
60 sec, pH4.5
30 sec, pH2
60 sec, pH2
E
final length [um]
initial length [um]
r=0.38
F
N
MSE Microns²
same
random

Figure S1

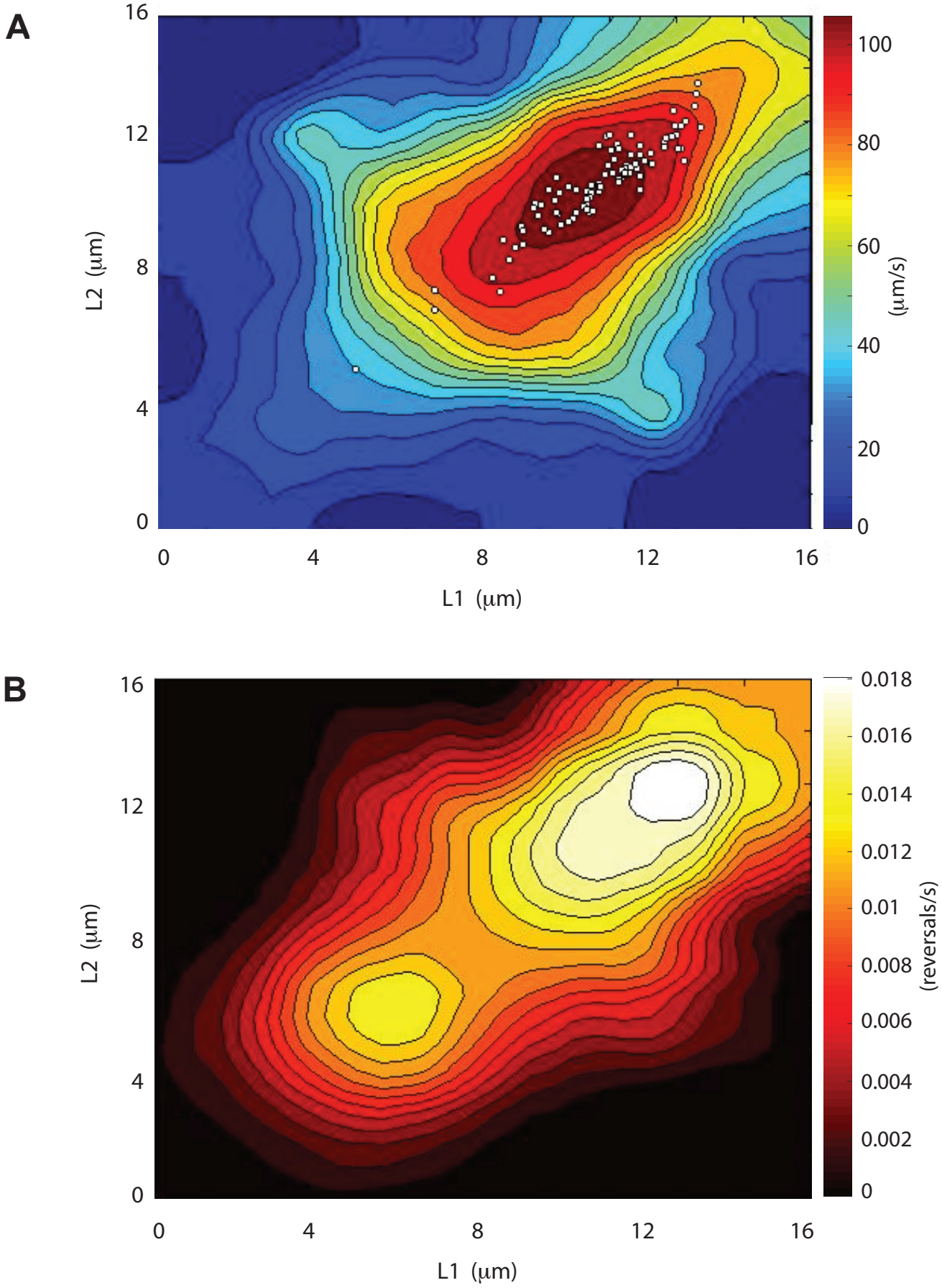
A
16
12
8
4
0
L2 (μm)
0
4
8
12
16
L1 (μm)
100
80
60
40
20
0
(μm/s)
B
16
12
8
4
0
L2 (μm)
0
4
8
12
16
L1 (μm)
0.018
0.016
0.014
0.012
0.01
0.008
0.006
0.004
0.002
0
(reversals/s)

Figure S2